Compositional Aspects of Iron Fischer–Tropsch Catalysts: An XPS/Reaction Study

C. S. KUIVILA, P. C. STAIR,[1] AND J. B. BUTT[2]

Ipatieff Laboratory, Northwestern University, Evanston, Illinois 60208

The catalytic and compositional behaviors of prereduced and unreduced iron catalysts for Fischer–Tropsch synthesis were investigated. Catalytic behavior was evaluated by measuring rates of hydrocarbon formation in a $3:1$ $H_2:CO$ mixture at 1 atm and 250°C. Iron phases which evolved near the catalyst surfaces were characterized by X-ray photoelectron spectroscopy, and bulk phases present following reaction were determined by Mössbauer spectroscopy. At low conversion levels the prereduced catalyst was gradually converted to iron carbide with no significant oxide phase formed. Synthesis activities increased initially with the formation of active surface carbon, but eventually lost some activity due to graphitic carbon formation. At higher conversions, the prereduced catalyst showed some formation of surface oxide phases and an inhibition of the synthesis rate due to water adsorption. Surface carbon accumulation was also suppressed under these conditions. Unreduced Fe_2O_3 showed no initial synthesis activity, but underwent a gradual activation to become even more active than the prereduced catalyst. The oxide catalyst was eventually completely reduced to Fe_3O_4, and any metallic phase formed was rapidly converted to iron carbide. Compared to reduced materials, the oxide catalyst accumulated considerably less surface carbon and showed no loss of activity for reaction times up to 48 h. XPS analysis suggests that Fe_3O_4 is active for synthesis. © 1989 Academic Press, Inc.

INTRODUCTION

It has been known since early studies of bulk-phase catalysts that iron is converted to one or more carbides under typical Fischer–Tropsch synthesis conditions. In fact, the working catalyst can consist of a mixture of metallic, carbide, and oxide phases; however, the role that these various phases play in the synthesis has not been resolved. Bulk-phase analysis has largely been based on Mössbauer (MES) and/or X-ray diffraction measurements of catalysts employed at low conversion levels, while surface studies have tended to focus on characterization of the carbon adlayer produced on the surface rather than the evolution of the various iron phases.

The present investigation was under-taken to provide a more integrated understanding of the compositional behavior of iron synthesis catalysts by comparing surface characterization as studied by X-ray photoelectron spectroscopy (XPS) with corresponding bulk characterization via MES. While the primary objective of the study was analysis of bulk and surface iron phases associated with synthesis activity, the work required development of an XPS spectrum fitting procedure, reported elsewhere (1).

BACKGROUND

Carburization. Carbide formation in reduced catalysts has received considerable attention in the recent literature, with techniques such as Mössbauer spectroscopy, X-ray diffraction, and thermomagnetic analysis being used to track the bulk iron phases developed during synthesis (2–5). For unsupported iron, mixtures of ε'-$Fe_{2.2}C$ and χ-Fe_5C_2 are formed during synthesis at

299

ca. 250°C, while cementite (θ-Fe$_3$C) appears at temperatures above 350°C (4). Studies of both supported (2, 6) and unsupported (5, 7, 8) catalysts have shown that the synthesis activity of reduced iron is initially low and increases to a maximum as carburization proceeds. Various models for this behavior have been proposed, but the so-called "competition model" (9) best explains most experimental observations (5, 8, 10, 11). Surface iron atoms are viewed as active sites, and the formation of both hydrocarbon products and bulk carbides involves a common carbon intermediate. During the early stages of synthesis, diffusion of carbon into the bulk is rapid, depressing the surface intermediate concentration. However, as carburization proceeds active carbon on the surface increases leading to higher hydrocarbon production. Specific evidence supporting this view has been reported by several workers (9, 12, 13).

Recent studies of Bianchi et al. (14, 15) point to two different forms of nongraphitic surface carbon. The more reactive of the two has a C/H ratio near unity, and hydrogenation of this form produces higher hydrocarbons as well as methane. The second, less reactive form consists primarily of carbon and has a surface concentration that passes through a maximum of synthesis proceeds. Hydrogenation of this form of surface carbon produces only methane. In an inert atmosphere at synthesis temperatures, the CH species is stable, while the carbon-rich species is gradually converted to bulk carbide. Thus, active CH is the precursor to methane and higher products, but represents only a fraction of the total carbon on the surface during synthesis.

A more direct interpretation of the relationship between synthesis activity and carburization assumes simply that the carbide is more active than iron, but this interpretation can be rejected for a number of reasons as discussed by Niemantsverdriet and van der Kraan (9). However, while it may be clear that carbides are not essential for development of synthesis activity per se, it is quite probable that catalyst behavior is significantly affected by the formation of surface carbide phases. In particular, carbide formation has been shown to enhance the competitive chemisorption of H$_2$ over CO (16).

Since it is generally agreed that water is a primary synthesis product (17), the high initial rate of dissociative CO chemisorption on iron dictates a correspondingly high initial rate of hydrogen consumption. Both of these effects suggest that a reduced catalyst surface will be hydrogen-deficient initially, with more surface hydrogen becoming available for product formation as carburization proceeds. This view of an increasing surface hydrogen concentration is also supported by the lower olefin/paraffin ratios observed for carbided catalysts (6, 10).

Oxide phases. Synthesis at higher conversions leads to significant oxidation of iron catalysts to Fe$_3$O$_4$. Shultz et al. (18) concluded that water was responsible for such oxidation. This is likely, since even at low conversions there is a strong interaction of water with iron surfaces (10, 14). Views in the literature regarding the catalytic contributions of oxides to synthesis activity are mixed. One model of synthesis over reduced iron proposes that maximum activity will be limited by the extent of oxidation to Fe$_3$O$_4$ since it is assumed that the oxide has no synthesis activity (19). More direct studies are reported by Reymond et al. (20) and Dictor and Bell (21, 22). The former report synthesis over an unreduced iron oxide to give hydrocarbon product distributions similar to that of reduced iron, with a maximum activity occurring over a material consisting of approximately equal amounts of magnetite and Hägg carbide. On a weight basis, this activity was about 50% higher than that of the reduced catalyst. Since further carbide formation in the unreduced catalyst coincided with a diminished rate of synthesis, it was concluded that Fe$_3$O$_4$ *is* an active catalyst for the syn-

thesis. In the latter, a similar study was carried out in a slurry-phase reactor using both reduced and unreduced Fe_2O_3 powder as the starting material. The formation of Hägg carbide and Fe_3O_4 was also observed for the unreduced powder after an extended time-on-stream, and similar product distributions for reduced and unreduced materials were reported. However, these workers concluded that the similar product distributions indicated a common active phase (i.e., Hägg carbide) and that Fe_3O_4 *is not* an active catalyst for the synthesis. This is pretty much where the matter stands at present.

Surface studies. The first surface studies on the iron Fischer–Tropsch system, making use of both XPS and Auger electron spectroscopy (AES), were those of Bonzel and co-workers (*23–25*) who studied polycrystalline foils or (110) orientation single crystals. They claimed identification of three forms of carbon on the surface at various stages in the synthesis: a CH_x "hydrocarbon" phase and a partially hydrogenated "carbidic carbon" early on, with a "graphitic carbon" phase growing in later. Carbidic carbon was associated with initial increases in synthesis activity and graphitic carbon with long-term decline. However, these model catalysts seem to be much more susceptible to deactivation resulting from rapid buildup of inactive surface carbon than do small iron particles. This may be due to cold-working of these materials during their preparation, which can lead to slower rates of carbon dissolution and/or carbide formation (*26*). The recent studies of Dwyer and Hardenbergh (*27, 28*) also demonstrate the nature of carbon buildup on foils and on moderate surface area (16 m^2/g) powders. For a foil the $C(1s)$ XPS spectrum exhibited equal intensity peaks for graphitic (284.6 eV) and carbidic (283.2 eV) carbon after reaction, while for a similarly treated powder sample, the spectrum was dominated by the carbidic carbon peak. A point of interest for the present study was the reported behavior of the

$Fe(2p_{3/2})$ peak, found at 706.6 eV for both forms of material before reaction. The shape of the spectrum was unchanged after synthesis, but a reproducible shift of the peak maximum to 706.9 eV was observed. This shift, coupled with the appearance of the low binding energy carbon peak, was attributed to the formation of a carbide phase within the surface region of the catalyst.

The objectives of the studies reported here were threefold. The first objective was to combine Mössbauer bulk analysis and quantitative XPS surface analysis to confirm that conclusions regarding the formation of carbide phases based on bulk characterization (Mössbauer) were relevant to the composition of the catalyst surface. Second, the influence of the catalyst precursor (reduced or unreduced Fe_2O_3) was examined by both Mössbauer and XPS in order to resolve whether or not Fe_3O_4 is active for synthesis. The final objective was to investigate the nature of surface phases present at higher conversion conditions since this regime is technologically important and has not been reported on previously.

EXPERIMENTAL

Catalysts. Synthesis reactions were carried out over a commercial Fe_2O_3 powder (Alfa Products, 99.9%), in both reduced and as-received oxide forms. The synthesis properties of an unpromoted precipitated catalyst and a 10% silica-supported catalyst were also studied. Results obtained from these materials were similar to those of the reduced, unsupported oxide and will not be discussed here. Hydrogen chemisorption was used to estimate the exposed iron surface areas (*10*), and the turnover frequencies reported here are based on the hydrogen uptakes of the reduced catalysts assuming two surface iron sites per adsorbed hydrogen molecule.

XPS measurements. These were performed in a modified AEI ES200 ESCA spectrometer equipped with a hemispheri-

cal electrostatic energy analyzer. Samples were introduced into the system through a small volume (ca. 30 cm³) reaction cell attached to the ultrahigh vacuum chamber via a miniature gate valve. All XPS samples were approximately 8 × 24 mm in size and mounted on a copper sample stage with beryllium–copper screws. Powder samples were prepared by pressing the materials into a 48-mesh copper screen. Spectra were obtained using Al $K\alpha$ X-rays (1486.6 eV), and binding energies were calibrated by comparison to the Au($4f_{7/2}$) line (84.0 eV) for a clean gold foil mounted on the back side of the sample stage.

Reaction measurements. The reaction system consisted of a conventional fixed-bed flow reactor with associated purification train (*10*) connected upstream from the XPS reaction cell. Activity studies were carried out in the flow reactor, normally at 2–5% CO conversion. Low conversion reactions with corresponding XPS measurements were conducted on samples in the ESCA reaction cell and higher conversion (30–40%) XPS/reaction studies involved connecting the two reactors in series with the bulk of the conversion taking place in the fixed-bed prereactor. In this configuration the XPS sample in the reaction cell effectively represented a small catalyst section at the end of an integral rector. All reactions were carried out at 1 atm and 250°C with a 3 : 1 H_2 : CO feed; reduction of Fe_2O_3 was at 1 atm in hydrogen (Matheson, 99.99%) at 400°C for 10–12 h. Product stream analysis via gas chromatography was similar to that of Amelse *et al.* (*10*) and included methane, CO_2, and C_2–C_5 hydrocarbons.

Mössbauer measurements. Bulk iron phases were determined via room temperature spectra of oxygen passivated material from both the fixed-bed and the reaction cell. The source consisted of ^{57}Co diffused into a rhodium matrix (New England Nuclear); other details of the spectrometer operation, detection, and data collection and analysis were as given by Matyi *et al.* (*29*).

Catalyst spectra were generally collected over a period of 2–4 days, with about 0.5 to one million counts being accumulated in each of the 512 MCA channels.

XPS characterization of iron phases. Investigation of the iron phases in a working catalyst is a complicated problem, since such materials include metallic iron, Fe(II) and Fe(III) species in iron oxides, and various iron carbides. Reference data and development of an interpretation method for XPS data on these systems, summarized here, are given in detail elsewhere (*1*).

Metallic iron and the stoichiometric oxides Fe_2O_3 and Fe_3O_4 are readily identified by their characteristic Fe($2p$) peak positions and additional satellite features (*1*). In measurements of oxide powder samples it is important to remove adsorbed water (1 h at 170°C *in vacuo* is normally sufficient) to obtain reproducible spectra. The Fe($2p$) spectrum of Fe_3O_4 has been shown to be well approximated by a weighted average of the spectra characteristic of Fe_2O_3 and Fe_xO (*30*). The O($1s$) binding energy for iron oxides is approximately 530.3 eV for all oxide phases, making this spectrum of little value in distinguishing among different phases. Graphitic and carbidic carbon were characterized by C($1s$) binding energies at 284.6 and 283.2 eV, respectively. The iron powders as carburized for XPS characterization consisted primarily of the χ-Fe_5C_2 phase (*1*). An Fe($2p_{3/2}$) binding energy of 707.0 eV was measured for the reduced iron samples, and a reproducible shift to 707.3 eV observed after carburization. Similar increases were determined for the Fe($3s$) and Fe($3p$) binding energies of the carbide relative to metallic iron.

Applications to Fischer–Tropsch synthesis require the characterization of mixed-phase iron surfaces. In this case the overall near-surface composition can be estimated by determining the relative area contributions of each iron phase to the Fe($2p$) XPS spectrum. A least-squares procedure which uses linear combinations of XPS standard spectra for the individual iron phases (Fe,
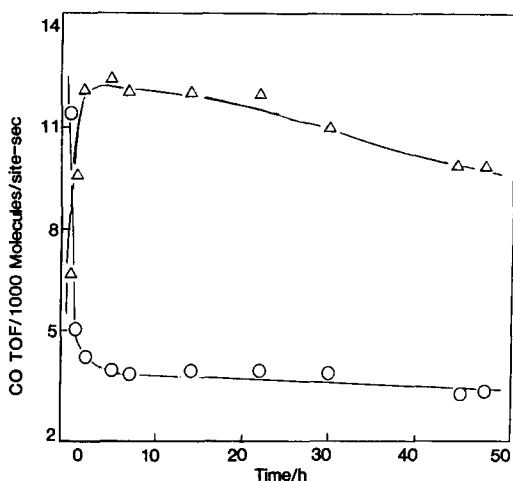
FIG. 1. CO turnover frequencies as a function of time for reduced iron oxide powder; △, to hydrocarbons; ○, to CO_2.

Fe(II), Fe(III), and Fe_5C_2) to fit spectra measured for mixed-phase surfaces was developed (*1*). The Fe(II) standard was obtained by subtracting out the Fe(III) contribution to the Fe_3O_4 spectrum. The resulting Fe(II) peak positions are in excellent agreement with literature XPS results (*30, 31*).

The primary sources of error involved in these determinations arise from the numerical procedures involved in determining spectral areas and experimental uncertainties associated primarily with the compositions of the standard spectra themselves. Details are discussed by Kuivila (*1, 32*); in the present work such errors sum to about 1% of the total spectral area. The contribution to this from the numerical procedure is <0.1%, which is the precision used in reporting spectral compositions.

Analysis via MES. Mössbauer characterization procedures were the same as those described previously (*2, 29*). Standard spectra were determined for the Fe_2O_3 and Fe_3O_4 powders as received, Fe_2O_3 after reduction for 10 h at 400°C (metallic iron) and after carburization in 3 : 1 H_2 : CO with the temperature increased gradually from 100 to 250°C over 95 h (Fe_5C_2). Spectral fits for these materials agreed with the literature

and the same samples were used to determine the XPS standard spectra; again, details are given by Kuivila (*1, 32*).

RESULTS

FIXED-BED REACTOR

Hydrogen Chemisorption

Hydrogen uptakes were measured for the reduced form of the Fe_2O_3 powder. The average over eight measurements was 15.5 μmol/g-cat. This translates into an average particle diameter of 430 nm.

Synthesis–Activities

Fixed-bed conversion experiments were carried out with the iron oxide powder in the as-received form and after prereduction in hydrogen. Specific rates are given as a function of reaction time for the two iron catalysts in Figs. 1 and 2 and selected data on conversion levels and rate values are given in Table 1.

The reduced oxide exhibited a gradual activation during the first 5 h, reaching a flat maximum for an extended period followed by a gradual loss of activity (Fig. 1). During the initial period, CO_2 formation exhibited a trend opposite to that for synthesis activity.
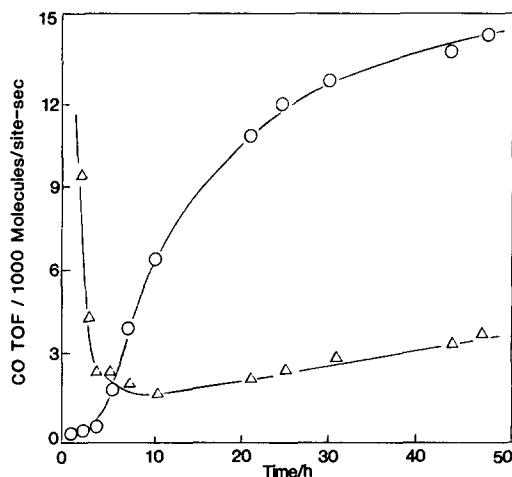

FIG. 2. CO turnover frequencies as a function of time for unreduced iron oxide powder; ○, to hydrocarbons; △, to CO_2.

TABLE 1

Synthesis Activity of the Iron Catalysts[a]

	Reduced oxide powder	Unreduced oxide
Figure	1	2
Rate[b]		
Average[c]	0.011	0.006
Maximum	0.012	0.015
Final[d]	0.010	0.015
Deactivation[e]	21	0

[a] Conversions of CO from 0 to 5%; 3 : 1 H_2:CO, 1 atm, 250°C.

[b] Molecules CO/site—sec to hydrocarbons.

[c] 0–48 h.

[d] At 48 h.

[e] To steady-state reaction level.

We take this to indicate an important role of Boudouard disproportionation of CO initially, else CO_2 formation would track hydrocarbon formation (i.e., via water gas shift), given that water is a primary product (17). The initially high CO_2 selectivity is also consistent with the picture of a hydrogen-deficient surface that does not allow for effective removal of oxygen via formation of water.

Deactivation of the reduced catalyst can be attributed to the formation of inactive surface carbon, as is detailed in the next section. In general there was good agreement between the activity of this catalyst and both a reduced precipitated iron catalyst and a reduced 10% Fe/SiO_2 supported catalyst as mentioned in the last section.

In contrast to the reduced catalyst, the unreduced oxide powder exhibited no significant synthesis activity during the first 3 h on stream (Fig. 2). For the sake of consistency, the specific reaction rates in Fig. 2 were calculated on the basis of hydrogen uptake of the reduced powder. Although this hydrogen uptake is not meaningful for the unreduced oxide, the reaction rates are put on a consistent basis (per gram of catalyst) with the reduced powder. After the first 3 h the activity of the unreduced cata-

lyst increased steadily for the remainder of the experiment. After 30 h the activity reached the level exhibited by the reduced powder and was still increasing after 48 h. As was the case for the reduced catalyst, the rate of CO_2 formation was initially high and decreased significantly during the first few hours of reaction.

Mössbauer Characterization

Room temperature MES were measured for the passivated catalysts after 48 h onstream. The spectrum for the prereduced catalyst was identical, with Hägg carbide (Fe_5C_2) clearly the dominant phase as expected (4). Details of this are given by Kuivila (32).

The spectrum of the unreduced catalyst (also after 48 h) was more complicated; the major feature was two partially overlapping six-line patterns characteristic of Fe_3O_4, but smaller peaks associated with metallic iron and the Hägg carbide were also evident. Mössbauer parameters obtained from the fit to this spectra are given in Table 2. As indicated in the table, about 82% of the spectral area was associated with Fe_3O_4, and the area ratio of B to A patterns obtained for this phase was 1.86, in good agreement with the literature (33). One may expect that under synthesis conditions the reduction of Fe_2O_3 would proceed sequentially to Fe_3O_4 and thence to metallic iron. From these data it also seems likely that the reduction of Fe_2O_3 is facile compared to that of Fe_3O_4,

TABLE 2

Mössbauer Parameters for the Unreduced Catalyst after Synthesis—Fixed-Bed Reactor Results

Phase	Site	IS (mm/s)	QS (mm/s)	H (kOe)	Area (%)
Fe_3O_4	A	0.20	0.12	489.2	81.9
	B	0.61	0.07	458.2	
Fe_5C_2	I	0.12	0.10	187.0	17.4
	II	0.19	−0.13	215.8	
	III	0.10	−0.04	96.5	
Fe		−0.03	0.00	332.1	0.7

since the catalyst consists primarily of stoichiometric Fe_3O_4 (on the basis of the B/A area ratio), and that the metallic phase once formed carburizes readily, as evidenced by the large carbide to metal area ratio in the spectrum.

XPS REACTOR

Activity–Selectivity Measurements

Near-surface composition changes of the catalysts were determined as a function of time-on-stream for both the prereduced and the unreduced forms of the oxide powder. Conversion levels were ~1%, and data were obtained over a 30-h period in a sequence of seven reaction exposures/XPS characterizations. Each exposure involved reaction for a time period ranging from 10 min to several hours; at the end of the specified time period the sample was cooled to 90°C under the reaction mixture, the cell evacuated, and the sample transferred into the UHV chamber for XPS analysis. After analysis, the sample was moved back into the reaction cell and the procedure repeated. It is important to demonstrate the similarity of reaction behavior in the XPS cell and the fixed-bed reactor if the surface characterizations are to be at all representative of actual behavior. In general there was remarkable agreement in terms of the magnitude and time dependence of the CO turnover frequencies measured in the XPS cell and those in the fixed-bed studies, given the fat that the latter were at somewhat higher (~5%) conversion. Reaction results for hydrocarbon formation in the XPS cell are shown in Fig. 3. The time frames for activation and deactivation were slightly shorter than in the fixed bed, which may be ascribed to the differing conversion levels and reactor geometries, but the essential features of the fixed-bed results were obviously maintained and not altered significantly by repeated interruptions of the reaction. CO_2 production also mirrored the fixed-bed results.

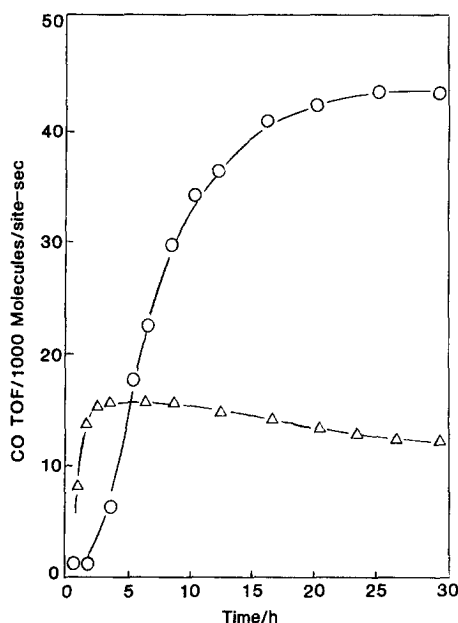Integral reactor studies in which the XPS

FIG. 3. CO turnover frequency as a function of time in the XPS cell at 1% conversion; ○, unreduced oxide powder; △, reduced oxide powder.

reactor cell was placed downstream of the fixed bed were also conducted. The effective conversion level seen by the XPS catalyst sample here was ~30–40%, providing a direct observation of product inhibition and surface composition at this level. The behavior of the prereduced oxide powder is shown in Fig. 4. Major features in comparison to low conversions are a much longer induction time, much lower activity levels probably due to product water on the surface, a pronounced increase in shift activity, and no significant deactivation.

XPS Characterizations

Survey spectra (32) revealed the presence of trace levels of sodium, carbon, sulfur, and silicon as impurities in the reduced catalyst; these were not thought to be present in sufficient quantities to influence the results obtained. Oxygen in the form of water or surface OH was also observed.

Reduced iron at low conversions. Changes in the near-surface iron phase composition were characterized by fitting
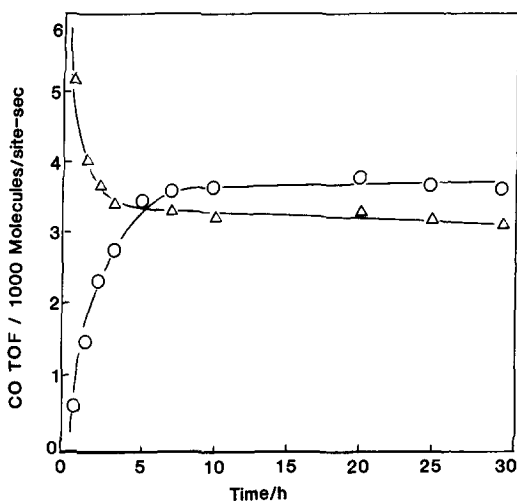
FIG. 4. CO turnover frequency for the reduced oxide powder at intermediate conversion (prereactor and XPS cell in series); $\bigcirc$, to hydrocarbons; $\triangle$, to CO_2.

the Fe(2p) spectrum using standard spectra characteristic of metallic iron, iron carbide, and the Fe(II) and Fe(III) oxide species. Typical results for the reduced materials after brief exposure to synthesis conditions are shown in Fig. 5. The entire Fe(2p) region (both $2p_{3/2}$ and $2p_{1/2}$ transitions) was included in the XPS analysis; only the

Fe($2p_{3/2}$) transition is shown in Fig. 5 in order to highlight the binding energy difference between metal and carbide transitions. Small oxide contributions, averaging about 0.3% Fe(2p) area for the reduced powder and 2.9% for the reduced, precipitated catalyst, which did not change over the entire time period investigated were observed.

Carbide contributions to the Fe(2p) spectra as a function of reaction time are plotted in Fig. 6. These are calculated as percentage of carbide associated with the reduced phase (metal plus carbide) on an oxide-free basis. Spectra for the reduced powder did not change appreciably after 10 h, although a small metallic iron contribution (ca. 3%) was maintained.

C(1s) measurements after various reaction times indicated that graphitic carbon increased steadily with time-on-stream. Graphitic and carbidic surface carbon formations during synthesis have been detailed by Deppe et al. (34) and Dwyer and Hardenbergh (27). Our results are in complete agreement with these previous studies.
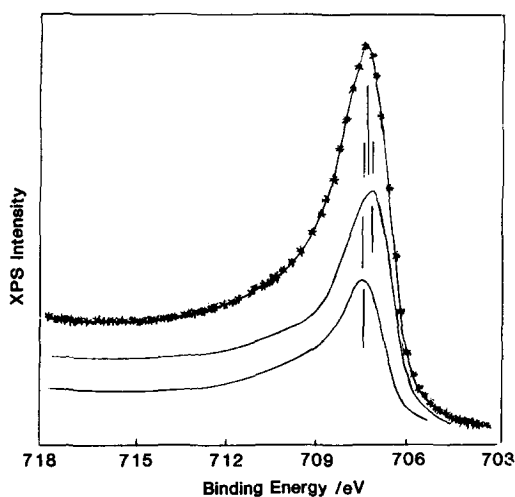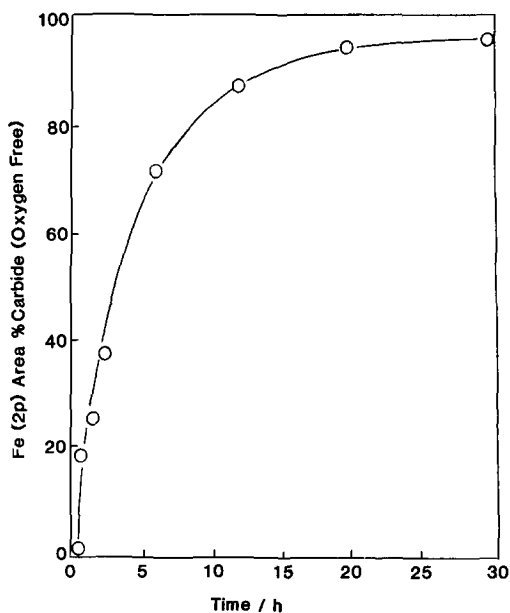

FIG. 5. Example of Fe(2p) spectrum fitting after synthesis for 2 h. The top curve is that experimentally observed. The second curve is for iron metal; the third for carbide. Overall composition of this sample was 62.4% metal, 37.4% carbide, and 0.2% oxide.

FIG. 6. Carbide contributions to the Fe(2p) XPS spectra of the reduced, unsupported catalysts as a function of time of reaction.
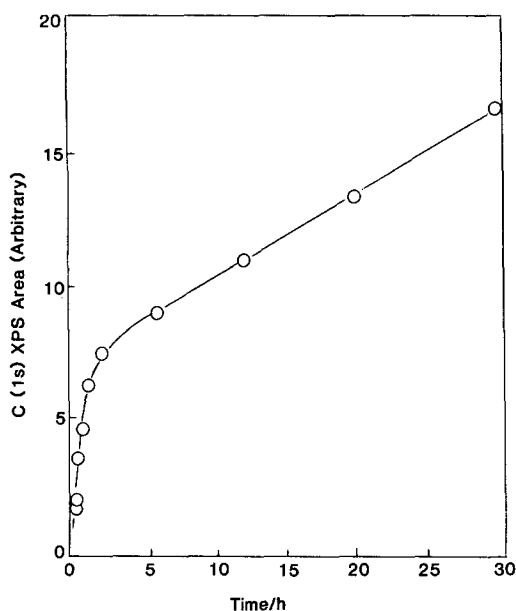
FIG. 7. C(1s) peak areas as a function of time of reaction for the reduced, unsupported catalysts.

The accumulation of carbon, represented in terms of total C(1s) area in Fig. 7, falls into two distinct regimes. Carbidic and graphitic surface carbon formed rapidly during the first few hours of synthesis, and this was followed by a remarkably constant rate of carbon deposition for the remainder of the run. The initial rapid accumulation of surface carbon coincides with increasing synthesis activity.

Iron oxide at low conversions. Core level iron XPS spectra measured during the course of reaction are shown in Fig. 8. It is seen that the initial oxide catalyst exhibited features characteristic of Fe_2O_3, with subsequent disappearance of the Fe(III) satellite peak at 719 eV and broadening of the parent peak signaling a partial reduction to divalent iron. The final spectrum, Fig. 8, bottom, is essentially that of Fe_3O_4. Note that there are no discernible metallic or carbidic contributions to these spectra. The O(1s) spectra (not shown) are dominated by an oxidic oxygen peak at 530.3 eV which steadily decreased in intensity over the reaction period, consistent with the behavior

of the iron spectra. A high binding energy shoulder on the oxygen spectra, indicative of water or OH on the surface, did not change significantly during the course of reaction.

Carbon core level measurements for the unreduced oxide were significantly different from those for the reduced materials. All C(1s) spectra were symmetric and relatively narrow (ca. 1.8 eV FWHM) with peak maxima corresponding to graphitic carbon (*32*). The absence of a significant carbidic contribution in these spectra was consistent with the minimal carbide phase detected in the fits to the Fe(2p) spectra. The C(1s) binding energy, at 285.1 eV, was slightly higher than that for the prereduced catalysts, but it is premature to conclude that this represents any real difference in the nature of the carbon formed on the unreduced surface, since differences in photoelectron relaxation energies could produce a shift of similar magnitude.

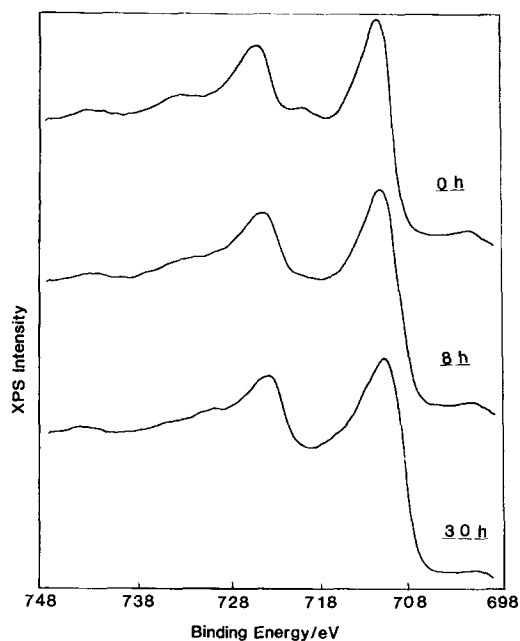A summary of the changes in near-surface composition for the unreduced pow-

FIG. 8. Fe(2p) spectra of unreduced oxide powder as a function of synthesis time.
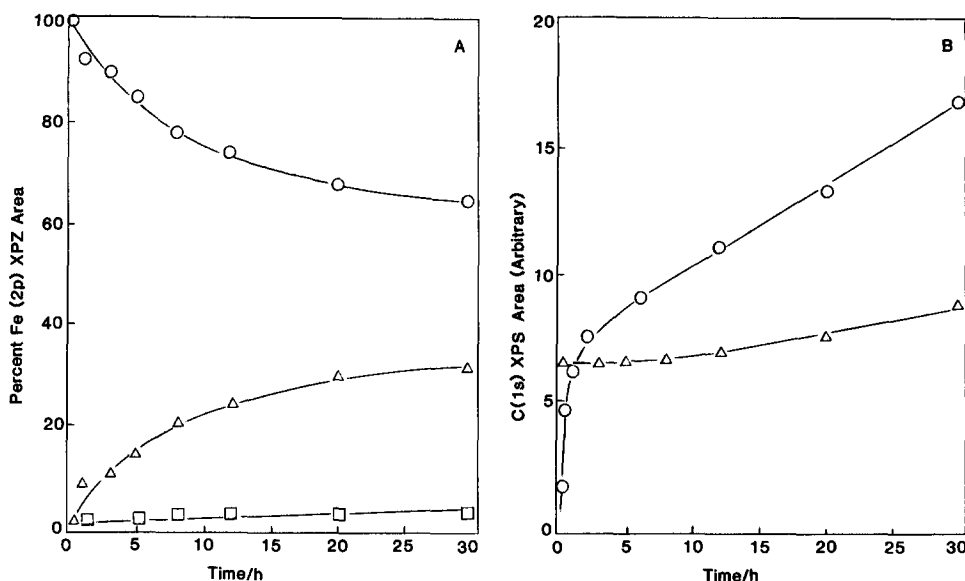
FIG. 9. (A) Survey of near-surface composition vs time of reaction for the unreduced oxide powder. O, Fe^{3+}; △, Fe^{2+}; □, carbide. (B) Comparison of C(1s) peak areas in reduced and unreduced catalysts; O, reduced oxide; △, unreduced oxide.

der, and a comparison of carbon buildup on reduced and unreduced materials are given in Fig. 9. It is seen in Fig. 9 that the rates of surface carbon accumulation are quite different for the reduced and unreduced materials. The higher synthesis activities observed for the initially unreduced catalyst at longer reaction times may be explained by a combination of the smaller amounts of inactive surface carbon and the steady activation resulting from progressive reduction from Fe_2O_3 to Fe_3O_4. The lack of a substantial carbide phase in the unreduced powder is consistent with the views of Reymond *et al.* (*20*) that Fe_3O_4 is active for synthesis; however, we do not agree with their conclusion that carbide formation is associated with the higher rate of deactivation of reduced iron catalysts, since the present studies confirm prior reports on the basis of bulk phase observations that the *activation* of reduced iron is clearly associated with carbide formation. Instead, it is clear that at low pressures reduced iron catalysts are more susceptible to the accumulation of

graphitic surface carbon (not carbide) which is responsible for their deactivation.

Reduced iron at intermediate conversions. Iron core level spectra for the prereduced powder after 10 and 30 h on stream are shown in Fig. 10. The CO conversion level "seen" by these catalysts was ~40% total, or ~20% to hydrocarbons. At these conversions there is an increase in the $Fe(2p_{3/2})$ binding energy of about 0.3 eV relative to the reduced starting material, indicating that carbide was still the major phase formed in the near-surface region. Small oxide contributions at ca. 711 eV are also observable in Fig. 10, but it is clear that catalyst oxidation was not significant. At low conversion (*32*) roughly 0.3% of the Fe(2p) area originated from oxides compared to about 2% at the higher conversions.

The rates of carbide formation at low and high conversion differed significantly. For example, after 10 h on-stream iron carbide accounted for 84% of the Fe(2p) area for the low conversion catalyst compared to
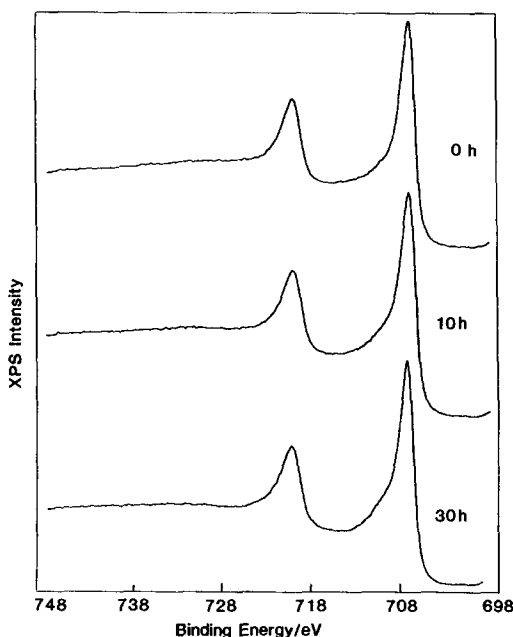
FIG. 10. Fe(2p) XPS spectra of the reduced oxide powder after various times under reaction conditions.

59% for the higher conversion material. Similar but smaller differences were observed at 30 h, but both catalysts appeared headed for about the same ultimate level of carbide, well above 95%. Slower carburization at higher conversions can be attributed to the same or similar product inhibition affecting overall synthesis rates.

An interesting comparison of low and intermediate conversion behavior was provided by the C(1s) spectra. After 30 h considerably less carbon is present on the higher conversion catalyst, and there is an obvious carbidic carbon peak at ~283.2 eV, indicating that relatively little graphitic carbon was present on the surface. In contrast, at low conversion graphitic carbon is the dominant C(1s) contribution during the entire course of reaction.

As might be expected from the oxide contributions to the Fe(2p) spectra, oxygen core level measurements did not provide much additional insight into the nature of the higher conversion surface. All O(1s) spectra obtained as a function of reaction

time were broad and centered around a binding energy of about 532 eV, indicative of water or surface OH, with only a small and poorly resolved oxidic contribution indicated.

Comparisons with Mössbauer Characterizations

Mössbauer spectra were also obtained for the samples characterized by XPS. The spectrum for the reduced catalyst was fit with four six-line patterns, corresponding to metallic iron and the Hägg carbide. It was similar to the spectrum obtained in the fixed-bed reactor study except that the metallic iron contribution was larger due to the shorter reaction time employed; the spectrum was also consistent with the XPS results.

An exception to this pattern of agreement between XPS and MES was provided by the unreduced oxide catalyst after reaction. The Mössbauer spectrum was well fit with five six-line patterns to account for the oxide and carbide phases (no metallic phase was evident), and the parameters of this fit, given in Table 3, are to be compared with those of Table 2. It is seen that iron carbide contributed nearly 22% of the MES spectral area for the unreduced XPS cell catalyst. While this is generally consistent with the fixed-bed results, there is a discrepancy with the Fe(2p) XPS results for the same material, which indicated only a small carbide contribution (~3%). Not only is the

TABLE 3

Mössbauer Parameters for the Unreduced Catalyst after Synthesis—XPS Cell Results (30 h)

Phase	Site	IS (mm/s)	QS (mm/s)	H (kOe)	Area (%)
Fe₃O₄	A	0.21	0.11	489.8	78.2
	B	0.61	0.07	458.6	
Fe₅C₂	I	0.17	0.00	186.2	21.8
	II	0.21	−0.16	214.3	
	III	0.11	−0.01	99.0	
Fe	—	−.03	0.00	332.1	0.0

magnitude of the difference surprising, so is its direction, since one would expect the carbide phase to form initially at the catalyst surface and any compositional enhancement would be found near the surface.

There are a number of possible experimental effects in the XPS measurements that could be postulated as leading to this discrepancy (32), but all seem unlikely. We must take this result at face value and then conclude that a significant and largely subsurface carbide phase is formed during synthesis on the unreduced oxide. Nucleation of a reduced phase below the catalyst surface (and subsequent carburization of that phase) is clearly not a reasonable expectation. More plausible is migration of the oxide over an iron carbide phase that did initially form on the catalyst surface. Water is known to enhance the mobility of oxide phases (35), and such mobility has been demonstrated for silica in supported iron shift catalysts (36) and strong evidence exists for other systems, notably iron–manganese oxide synthesis catalysts (37, 38). At this point we can add only the present results to the list of circumstantial evidence; this is certainly a fine area for further investigation.

SUMMARY

(1) At low conversions the surface of prereduced unsupported iron is gradually converted to carbide; no significant oxide phases are formed. Early activation is accompanied by a high rate of surface carbon accumulation and the near-surface region is rapidly converted to carbide. At longer reaction times surface carburization rates decrease but surface carbon continues to accumulate. This continued accumulation results in loss of activity.

(2) At higher CO conversions (~40% total) iron carbide is still the dominant surface phase formed in prereduced catalysts; oxide phases are present but in small amounts. The rate of carbon accumulation is depressed under these conditions and the surface carbon tends to be carbidic in nature.

(3) Unreduced Fe_2O_3 powder exhibits no initial synthesis activity but undergoes activation to Fe_3O_4 with an activity higher than the corresponding prereduced powder (weight basis). The reduction of Fe_2O_3 to Fe_3O_4 is a relatively facile step compared to subsequent reduction to metallic iron. Once formed, the metallic phase is rapidly converted to carbide. Compared to the prereduced form the unreduced powder accumulates considerably less surface carbon and has a lower rate of deactivation. XPS results strongly suggest that Fe_3O_4 is active for synthesis in support of the view held by Reymond et al. (20) and in contradiction to the conclusions of Dictor and Bell (21, 22).

(4) There is general agreement between catalyst compositions determined by XPS and MES with the exception of the unreduced oxide powder following reaction. It appears in the latter case that the carbide phase detected by MES is below the catalyst surface while the surface consists primarily of Fe_3O_4.

REFERENCES

1. Kuivila, C. S., Butt, J. B., and Stair, P. C., Appl. Surf. Sci. 32, 99 (1988).
2. Amelse, J. A., Butt, J. B., and Schwartz, L. H., J. Phys. Chem. 82, 558 (1978).
3. Raupp, G. B., and Delgass, W. N., J. Catal. 58, 348 (1979).
4. Niemantsverdriet, J. W., van der Kraan, A. M., van Dijk, W. L., and van der Baan, H. S., J. Phys. Chem. 84, 3363 (1980).
5. Sancier, K. M., Isakson, W. E., and Wise, H., Adv. Chem. 178, 129 (1979).
6. Raupp, G. B., and Delgass, W. N., J. Catal. 58, 361 (1979).
7. Matsumoto, H., J. Catal. 86, 201 (1984).

8. Matsumoto, H., and Bennett, C. O., *J. Catal.* **53**, 331 (1978).
9. Niemantsverdriet, J. W., and van der Kraan, A. M., *J. Catal.* **72**, 385 (1981).
10. Amelse, J. A., Schwartz, L. H., and Butt, J. B., *J. Catal.* **72**, 95 (1981).
11. Reymond, J. P., Meriaudeau, P., Pommier, B., and Bennett, C. O., *J. Catal.* **64**, 163 (1980).
12. Ott, G. L., Fleisch, T., and Delgass, W. N., *J. Catal.* **65**, 253 (1980).
13. Dwyer, D. J., and Somorjai, G. A., *J. Catal.* **52**, 291 (1978).
14. Bianchi, D., Borcar, S., Teule-Gay, F., and Bennett, C. O., *J. Catal.* **82**, 442 (1983).
15. Bianchi, D., Tau, L. M., Borcar, S., and Bennett, C. O., *J. Catal.* **84**, 358 (1983).
16. Podgurski, H. H., Kummer, J. T., DeWitt, T. W., and Emmett, P. H., *J. Amer. Chem. Soc.* **72**, 5382 (1950).
17. Dry, M. E., Shingles, T., and Boshoff, L. J., *J. Catal.* **25**, 99 (1972).
18. Schultz, J. F., Hall, W. K., Seligman, B., and Anderson, R. B., *J. Amer. Chem. Soc.* **77**, 213 (1955).
19. Hojlund-Nielsen, P. E., and Bogild-Hansen, J., *J. Mol. Catal.* **17**, 183 (1982).
20. Reymond, J. P., Meriaudeau, P., and Teichner, S. J., *J. Catal.* **75**, 39 (1982).
21. Dictor, R. A., and Bell, A. T., *J. Catal.* **97**, 121 (1986).
22. Dictor, R. A., and Bell, A. T., *Prepr. ACS Div. Pet. Chem.* **31**, 126 (1986).
23. Krebs, H. J., Bonzel, H. P., and Gafner, G., *Surf. Sci.* **88**, 269 (1979).
24. Bonzel, H. P., and Krebs, H. J., *Surf. Sci.* **91**, 499 (1980).
25. Krebs, H. J., and Bonzel, H. P., *Surf. Sci.* **99**, 570 (1980).
26. Emsley, A. M., and Hill, M. P., *Carbon* **15**, 205 (1977).
27. Dwyer, D. J., and Hardenbergh, J. H., *J. Catal.* **87**, 66 (1984).
28. Dwyer, D. J., and Hardenbergh, J. H., *Appl. Surf. Sci.* **19**, 14 (1984).
29. Matyi, R. J., Butt, J. B., and Schwartz, L. H., *J. Catal.* **91**, 185 (1985).
30. Wandelt, K., *Surf. Sci. Rep.* **2**, 1 (1982).
31. Oku, M., and Hirokawa, K., *J. Appl. Phys.* **50**, 6303 (1979).
32. Kuivila, C. S., Ph.D. dissertation, Northwestern University, 1987. Available from University Microfilms, Inc.
33. Lund, C. R. F., and Dumesic, J. A., *J. Phys. Chem.* **85**, 3175 (1981).
34. Deppe, P., Papp, H., and Baerns, M., *Hyperfine Interact.* **28**, 903 (1986).
35. Anderson, J. R., "Structure of Metallic Catalysts." Academic Press, New York, 1975.
36. Lund, C. R. F., and Dumesic, J. A., *J. Catal.* **72**, 21 (1981).
37. Kreitman, K. M., Baerns, M., and Butt, J. B., *J. Catal.*, in press.
38. Jensen, K. B., and Massoth, F. E., *J. Catal.* **92**, 98 (1985).